

Article

Assessing Regional Climate Models (RCMs) Ensemble-Driven Reference Evapotranspiration over Spain

Patricia Olmos Giménez and Sandra G. García-Galiano * 

Department of Civil Engineering, R&D Group of Water Resources Management, Universidad Politécnica de Cartagena, Paseo Alfonso XIII, 52, 30203 Cartagena, Spain; patricia_olmos@live.com

* Correspondence: sandra.garcia@upct.es; Tel.: +34-968-325-935

Received: 30 May 2018; Accepted: 1 September 2018; Published: 4 September 2018



Abstract: The present work applies a novel methodology of combining multiple Regional Climate Models (RCMs) (or ensemble) that are based on the seasonal and annual variability of temperatures over Spain, which allows for the quantification and reduction of uncertainty in the projections of temperature based-potential evapotranspiration. Reference evapotranspiration (ET_0) is one of the most important variables in water budgets. Therefore, the uncertainties in the identification of reliable trends of reference evapotranspiration should be taken into account for water planning and hydrological modeling under climate change scenarios. From the results over Spain, the RCMs ensemble reproduces well the yearly and seasonal temperature observed dataset for the time reference period 1961–1990. An increase in the ensemble-driven ET_0 for time period 2021–2050 over Spain is expected, which is motivated by an increase in maximum and minimum temperature, with the consequent negative impacts on water availability.

Keywords: regional climate models; PDF ensembles; reference evapotranspiration; climate change; Spain

1. Introduction

Projecting the impacts of climate change on temperature and rainfall has become an important issue [1–3]. Besides precipitation, potential evapotranspiration (PET) is the most important variable for determining the water balances at different spatial scale (e.g., basin, region).

Reliable PET projections are needed for hydrologic modelling under climate change scenarios. However, in order to evaluate its impact on water balances, PET can only be estimated indirectly, i.e., by considering some other directly measurable weather elements currently obtained by climatic models [4].

It is remarkable that PET is considered equivalent to the reference evapotranspiration ET_0 by several authors [5–7], being assumed as the evapotranspiration rate of a short green crop (grass), completely shading the ground, of uniform height, and with adequate water availability in the soil profile. The main ambiguities and limitations with PET is that many types of crops can fit into the description of a short green crop. Conversely, the concept of reference evapotranspiration ET_0 [8] is better suited for agronomical purposes and it refers to the evapotranspiration from a standardized vegetated surface (with an assumed crop height of 0.12 m, a fixed surface resistance of $70 \text{ s}\cdot\text{m}^{-1}$ and an albedo of 0.23), well-watered grass of uniform height, actively growing, and completely shading the ground. Under these fixed conditions, the evaporative demand of the atmosphere can be considered to be independent of crop type, crop development, and management practices and dependent by meteorological conditions only.

ET_0 (and the consequent ET_c —maximum crop evapotranspiration) largely affects agricultural productivity. A reliable estimate of ET_0 in agricultural regions is highly valuable for implementing water management practices that will improve yields and promote sustainable agricultural practices [9,10]. Moreover, it is a very important issue in areas affected by water scarcity and droughts. Currently, this concept is used in hydrology as a robust input parameter to model at basin scale [11]. Moreover, the concept of ET_0 is interesting to define the values of evapotranspiration that were measured under different climates [12]. Consequently, special attention should be taken in the estimation of precipitation, ET_0 and their interactions.

The Penman-Monteith (PM) equation [13], which was adopted by the Food and Agriculture Organization (FAO), has been agreed as the standard model to estimate reference evapotranspiration (ET_0). However, the high requirement of meteorological variables (i.e., air temperature, relative humidity, solar radiation, and wind speed) represents a barrier in its application (specifically in areas where these meteorological variables are not currently measured). Therefore, these requirements constitute disadvantages in comparison with other methods with a less number of parameters [4].

Djaman et al. [14] applied sixteen ET_0 equations with a lower requirement of meteorological variables, when the weather datasets were scarce. Various authors [15–17] have demonstrated that radiation-based methods are appropriate for estimating ET_0 . The Hargreaves-Samani equation [18] constitutes an alternative model, when only air temperature and radiation datasets are available. Tabari [15] has checked that the Hargreaves-Samani equation turned out to be the most precise model under warm humid and semi-arid climatic conditions. However, other authors [19,20] have suggested overestimations of ET_0 when Hargreaves-Samani equation is applied in humid regions with a low ET rate, and underestimations in dry regions with high ET rate. To solve this issue, various authors [21–25] have proposed local adjustments of Hargreaves-Samani equation to improve its performance. In a recent study Tegos et al. [26] have shown that using a parametric model with explanatory variables temperature and extraterrestrial radiation, and parameters that are estimated through calibration, satisfactory PET results are obtained for the climate regime of Spain.

The maximum and minimum temperatures are required to estimate ET_0 projections that are based on the Hargreaves-Samani equation. Regional Climate Models (RCMs) are increasingly used to assess the impact of climate change. Due to biases that are associated with climate models projections, the combination of information provided by an ensemble approach from different RCMs simulations instead of only one specific RCM [27–30], is a way to reduce the involved uncertainties.

An ensemble approach has been recently used by [31,32] that is based on sixteen RCMs to generate rainfall and temperature projections. On the other hand, Xu et al. [33] have obtained projections of temperature and precipitation over China, under the Representative Concentration Pathways (RCP) scenarios, from an average of eleven Global Climate Models (GCMs). Diallo et al. [34] have suggested that multi-model RCM ensemble of temperature and precipitation based on different driving GCMs, help to compensate systematic errors from both the nested and the driving models.

Different works can be found in the literature oriented to assess the climate change on PET using RCMs or GCMs. Prudhomme et al. [6] have compared the future changes of PET from 12 equations in Great Britain with a RCM, getting a large variation in the magnitude of changes. Zhang et al. [35] have assessed the future change of ET_0 over China, from three GCMs under IPCC SRES A1B and B1 scenarios, demonstrating the expected important increases of ET_0 . Obada et al. [36], working with three RCMs in West Africa, have demonstrated gradual increases of annual PET until 2100, for the RCP4.5 and RCP8.5 scenarios.

Nevertheless, in almost all studies, the ability of RCMs in evaluating climate variables has been focused on precipitation and temperature, but not in the estimate of ET_0 . Moreover, in almost all studies of RCM-driven ET_0 the authors do not consider an ensemble of climate models. For this reason, the RCMs ensemble driven- ET_0 based on a locally calibrated simple model (like as Hargreaves-Samani equation), is paving the way in the reduction of involved uncertainties for projecting future changes.

In this paper, an indirect method to take into account the bias (or systematic errors) of temperature values has been applied. The simulated projections by RCMS with higher bias in relation to the historical dataset were penalized (less weight was given to them in the ponderation equation). The building of RCMS ensemble from a large number of climate model, has been based on a performance evaluation to reproduce the historical period (1961–1990). To reach this objective, a novel approach that was proposed by Olmos Giménez et al. [31] to calculate the reliability factor has been applied to build the maximum and minimum temperature ensembles from the RCMS projections. The methodological approach is evaluated based on its ability to reproduce the spatial and seasonal variability of temperatures for the baseline period 1961–1990. The estimated changes of ET_0 and temperature values between the baseline period and future period 2020–2050 are discussed. The main aim of this work is to improve the RCMS driven- ET_0 estimations over Spain, for increasing the reliability of water availability projections over continental Spain.

2. Material and Methods

2.1. Study Area and Datasets

The study area is located in continental Spain (Figure 1). The climate of Spain varies across the country, according to geographical situation and orographic conditions. When considering the climatological regimes of continental Spain, three zones are delimited (Figure 1) to study the impacts of climate change on ET_0 . From Figure 1, Zone 1 corresponds to Cantabrian coast, while Zone 2 is named Levante region (east of continental Spain); and, Zone 3 corresponds to the south of Spain (Andalusian region). The Northern part of Spain (especially the regions of Basque Country, Asturias, Cantabria, and Galicia) presents an oceanic climate characterized by mild winters and warm summers. The climate and landscape are determined by the Atlantic Ocean winds whose moisture gets trapped by the mountains circumventing the Spanish Atlantic coast.

The Mediterranean climate is characterized by two wet periods, spring and autumn, separated by hot and dry summers. The summer months present high evaporation and only occasional rainy events. High intensity rainfall events are usually recorded in autumn season. The south eastern part of Spain (mainly in region of Murcia and south of Valencian community) presents a semiarid climate. In contrast to the Mediterranean climate, the dry season continues beyond the end of summer season.

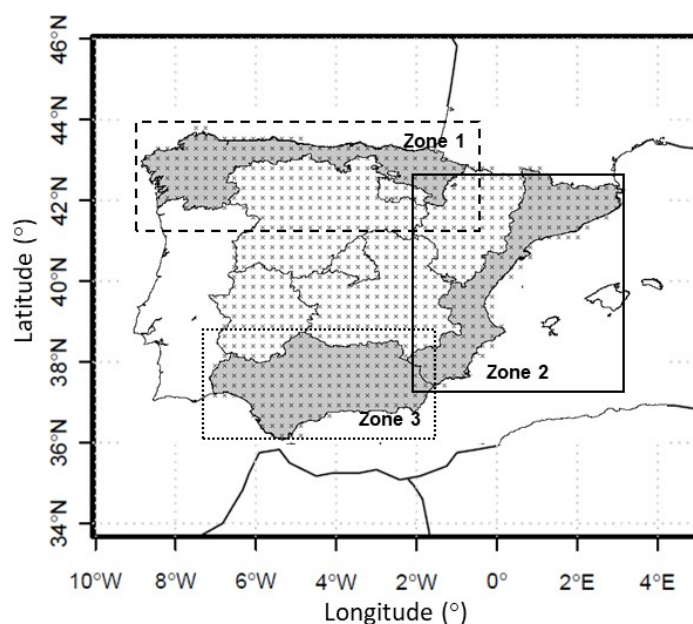


Figure 1. Map of location of 906 sites and study zones (Zone 1, Zone 2, and Zone 3) of continental Spain.

Observational grids of daily maximum and minimum temperature for Spain, have been obtained from the dataset named Spain02 (V2.1 version) from University of Cantabria (Santander, Spain) [37]. This dataset presents 0.2° of spatial resolution, for the time period 1961–2007.

The RCMs have been provided by the European project ENSEMBLES [38], with spatial resolution 0.25° , while considering the emissions scenarios that are described in the Special Report on Emission Scenarios of the IPCC [39]. A grid with 906 sites (or grid points) over Spain (Figure 1), has been considered to evaluate and validate the RCMs performances to build the ensemble of temperatures. The selected RCMs for scenario A1B [39] with a spatial resolution of 0.25° over continental Spain in the time period 1961–2050 have been: C4IRCA3, CNRM/RM5.1, DMI/ARPEGE, DMI/ECHAM5-r3, DMI/BCM, ETHZ/CLM, ICTP/REGCM3, KNMI/RACMO2, METNO/BCM, METNO/HADCM3Q0, MPI-M/REMO, OURANOS/MRCC4.2.1, SMHI/BCM, SMHI/ECHAM5-r3, SMHI/HadCM3Q3, and UCLM/PROMES.

2.2. Building the PDFs Ensemble

In the present work, an approach based in the reliability ensemble averaging (REA) method [29,40], already validated for ensembles of rainfall over Spain by Olmos Giménez et al. [31], has been implemented to address some limitations of the original approach. The upgrade essentially is oriented to modify the weights estimation method. Firstly, the convergence-based reliability factor of the original method was not considered, since it introduces great uncertainty. Secondly, the bias analysis was improved by considering the bias assessment for yearly and seasonal scales. The bias evaluates the performance of the model in reproducing the present climate (period 1961–1990). The assessment of the reliability factor is considered as an indirect way to take into account the bias, because the projections of RCMs with greater bias present less weight in the ponderation equation.

To calculate the reliability factor (R_i), the following equation is applied [31,32]:

$$R_i = \left(R_{Winter} R_{Spring} R_{Summer} R_{Autumn} R_{Yearly} \right)^{1/5}, \quad 1 \leq i \leq \text{number of RCMs} \quad (1)$$

where the factors R_{Winter} , R_{Spring} , R_{Summer} , R_{Autumn} , and R_{Yearly} measure the model's ability to reproduce each selected variable (in this case, the mean, maximum, and minimum temperatures) for the time reference period 1961–1990. These factors are calculated, as follows: firstly, the corresponding time series are extracted for each site (pixel of RCMs grid) both from the RCMs and observed datasets (906 sites over Spain). Secondly, seasonal and yearly cumulative density probabilities functions (CDFs) are fitted to the corresponding time series (from RCMs and observed dataset). The Weibull plotting position formula has been used to estimate the CDF. Thirdly, to measure the goodness of fit among the CDFs of observed dataset and RCMs, the p value of two-sample Smirnov-Kolmogorov test (TSSK) [41] is applied following the methodological approach that was proposed by Giraldo Osorio and García Galiano [3]. The TSSK test evaluates the similarity between the probability density functions that are associated with two independent samples, quantifying the maximum distance between the CDFs. The R value is obtained on each site (906 sites over continental Spain), then an interpolation method has been applied to obtain the spatial distribution. The R_i values varies from 0 to 1, where $R_i = 1$ represents the highest reliability.

The maps of normalized reliability factor (Pm) have been calculated with the equation that was proposed by [40] for each RCM in function of R_i .

$$Pm_i = R_i / \sum_{i=1}^N R_i \quad (2)$$

where $i = 1$ to N , and N is the number of RCMs.

Then, the PDFs ensembles have been obtained for the time period 2021–2050, while using P_m as the weighting factor of the RCMs. The process of building PDFs ensembles is explained in detail by [31].

2.3. Assessing Spatio-Temporal Distributions of ET_0

The estimation of spatio-temporal distribution of ET_0 has been performed from the observational dataset (time period 1961–1990), and from the RCM ensemble (time periods 1961–1990 and 2021–2050).

The equation that was proposed by Hargreaves and Samani (1985) [18] to estimate ET_0 is expressed, as follows,

$$ET_0 = CR_a(T_m + 17.8)(T_{max} - T_{min})^{0.5} \quad (3)$$

where ET_0 is the reference evapotranspiration (mm day^{-1}); R_a is the water equivalent of the monthly-averaged daily extraterrestrial radiation (mm day^{-1}), obtained from $R_a = 37.6 dr (\omega \sin\varphi \sin\delta + \cos\varphi \cos\delta \sin\omega)$, according to [13] where $1 \text{ mm day}^{-1} = 0.408 \text{ MJ m}^{-2} \text{ day}^{-1}$; dr is the inverse relative distance Earth-Sun; ω is the hour angle (rad); φ is the latitude (rad); δ is the solar declination (rad); T_{max} and T_{min} are the monthly-averaged maximum and minimum values of daily air temperature ($^{\circ}\text{C}$); and T_m is the monthly-averaged daily temperature, calculated as the average of T_{max} and T_{min} ; and, C is the Hargreaves coefficient, which original value is 0.0023. In this work, a calibrated coefficient (C') to southeast of Spain by Maestre Valero et al. (2013) [23] has been considered, with $C' = 0.00285$. The coefficient used is slightly higher than that of Hargreaves because southeast of Spain is considered to be a semiarid region, where original Hargreaves coefficient presents underestimations.

The Equation (4) adjusted to the Southeast of Spain [23] has been finally applied, as follows,

$$ET_0 = C'R_a(T_m + 17.8)(T_{max} - T_{min})^{0.5} \quad (4)$$

3. Results

3.1. RCMs Ensemble

In this work, the RCM ensemble for the mean, maximum, and minimum monthly temperatures variables have been obtained. The spatial distributions of values of reliability factor (R_i), built by applying the TSSK p value for mean temperature, are presented in Figure 2. These maps give a general idea about the reliability of each RCM to simulate the temperatures.

From Figure 2, the models with best performance to replicate the mean temperature have been DMI/ECHAM-r3, ETHZ/CLM, KNMI/RACMO2, METNO/HadCM3Q0, and MPIM/REMO. While, the models with worst performances have corresponded to OURANOS/MRCC4.2.1, DMI/BCM, SMHI/BCM, METNO/BCM, and SMHI/HadCM3Q3, presenting the lowest values of R over Spain. One of the RCMs (MPIM/REMO) presents an outstanding performance according to the R factor, although this model does not capture with enough reliability the observed patterns in the southwest corner of Spain. However, there are other models, such as DMI/BCM and DMI/ECHAM-r3, which present a good reliability in that area (southwest corner of Spain).

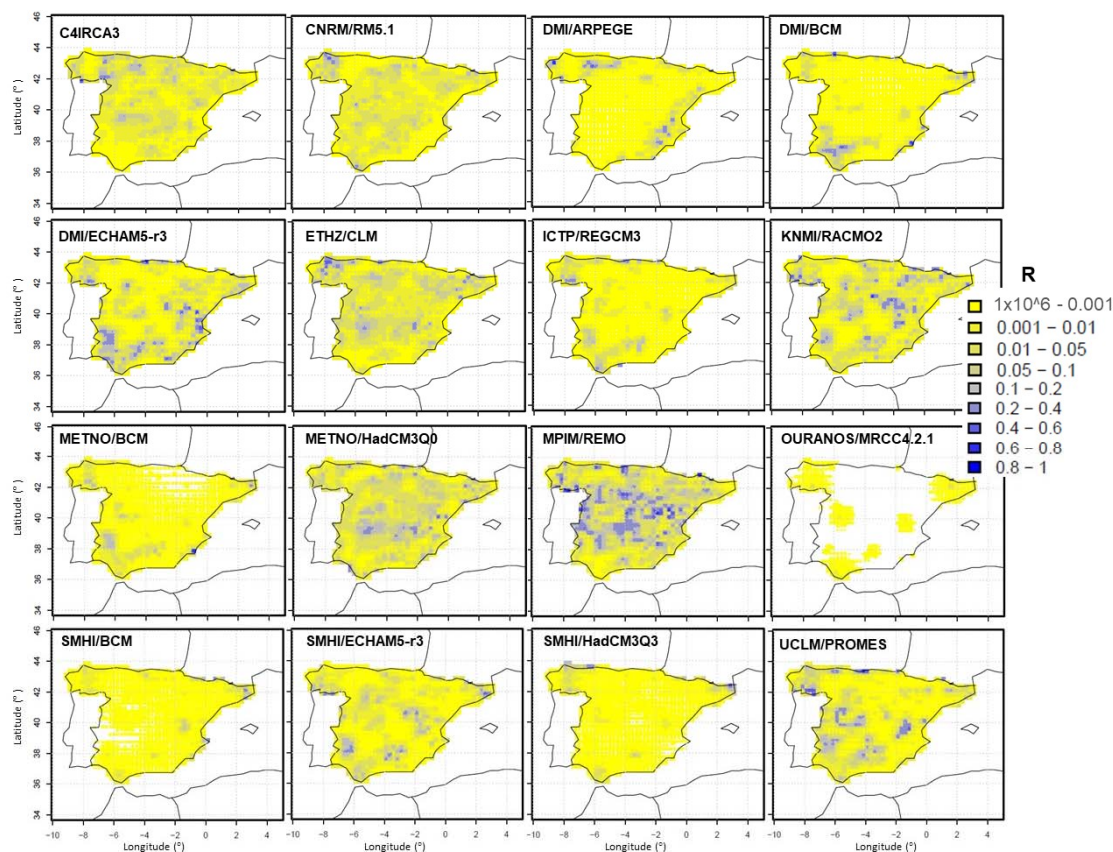


Figure 2. Maps of R values for average temperature, estimated by applying the Smirnov-Kolmogorov test (two-sample Smirnov-Kolmogorov test (TSSK) p value) for each Regional Climate Models (RCM).

Once P_m maps have been calculated for each RCM, the PDF ensemble for each site of the study area has been built. Monthly maps of mean, minimum, and maximum temperature for the periods 1961–1990 and 2021–2050, have been obtained.

The CDFs of mean, maximum and minimum temperature for the time reference period 1961–1990 have been obtained from observed dataset and RCMs. The CDFs and CDF ensemble that was obtained on site 36 (North of Spain) for each season and yearly mean temperature are presented in Figure 3 as a representative example, since the performance varies for each site and RCM. From Figure 3, it can be seen that CDF ensemble presents good performance with respect to observed data CDF. The best performance occurs for yearly mean temperature (0.765 p value). However, the best performances vary for each analyzed season, sites, and variables.

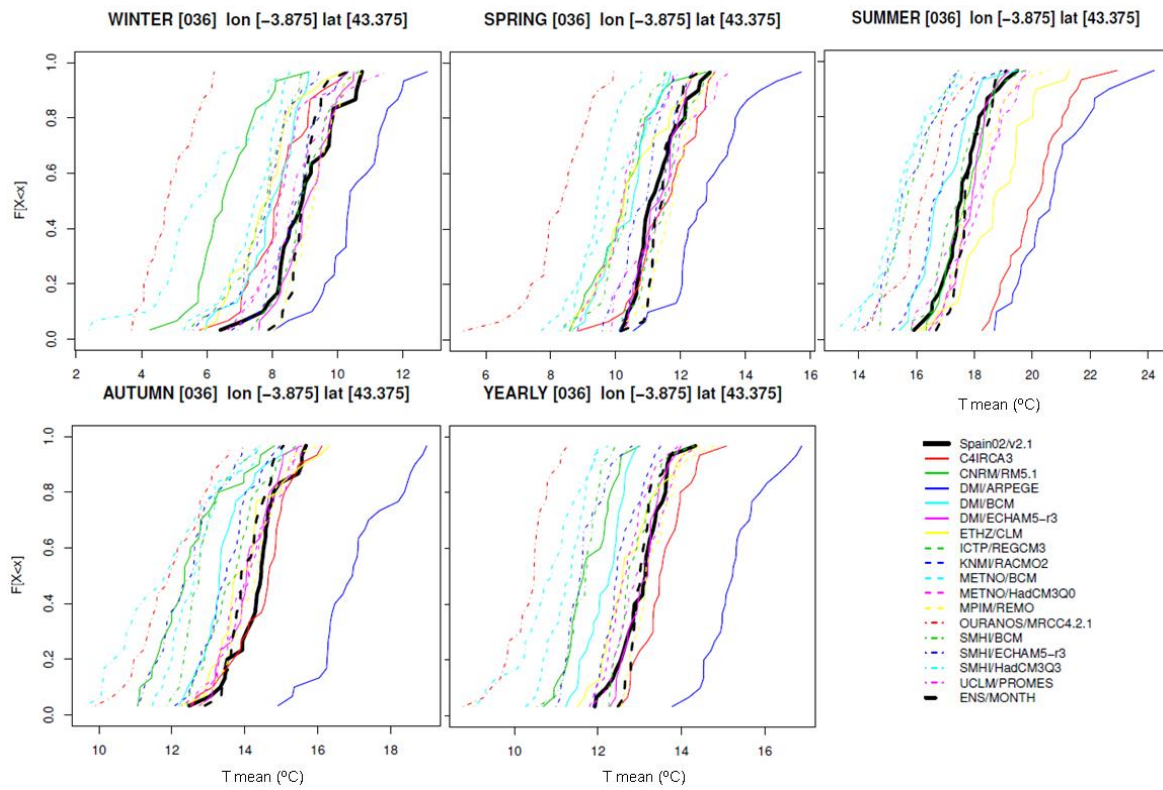


Figure 3. Cumulative density probabilities functions (CDFs) of mean temperature on site 36 from observed dataset (in black), ensembles (dashed black), and RCMs (in colour), for time reference period 1961–1990.

3.2. Assessing the Plausible ET_0 and Temperature Scenarios for 2021–2050

The ET_0 values applying the Equation (4) has been computed for each grid cell over Spain. Time series of ET_0 are calculated for the period 2021–2050 once the RCMs temperature ensembles have been obtained. Figure 4 presents the standardized monthly ET_0 and maximum and minimum temperature for the period 2021–2050. Positive trend in the three variables is evident from the Figure 4.

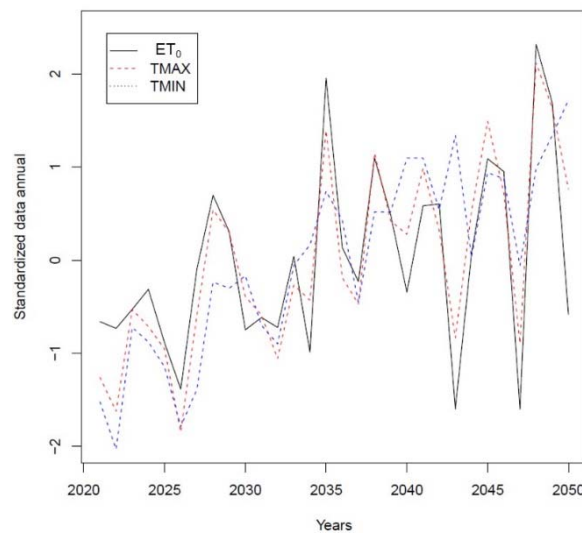


Figure 4. Standardized monthly data over continental Spain of RCM ensembles of ET_0 and maximum and minimum temperature for time period 2021–2050.

It is important to know the expected trends of both *ET₀* and temperatures. Therefore, the maps of RCM ensemble of mean annual *ET₀* and maximum and minimum temperature for the period 2021–2050 and scenario A1B (Figure 5a,c,e), and the variation with respect to the time reference period 1961–1990 over Spain (Figure 5b,d,f), have been evaluated.

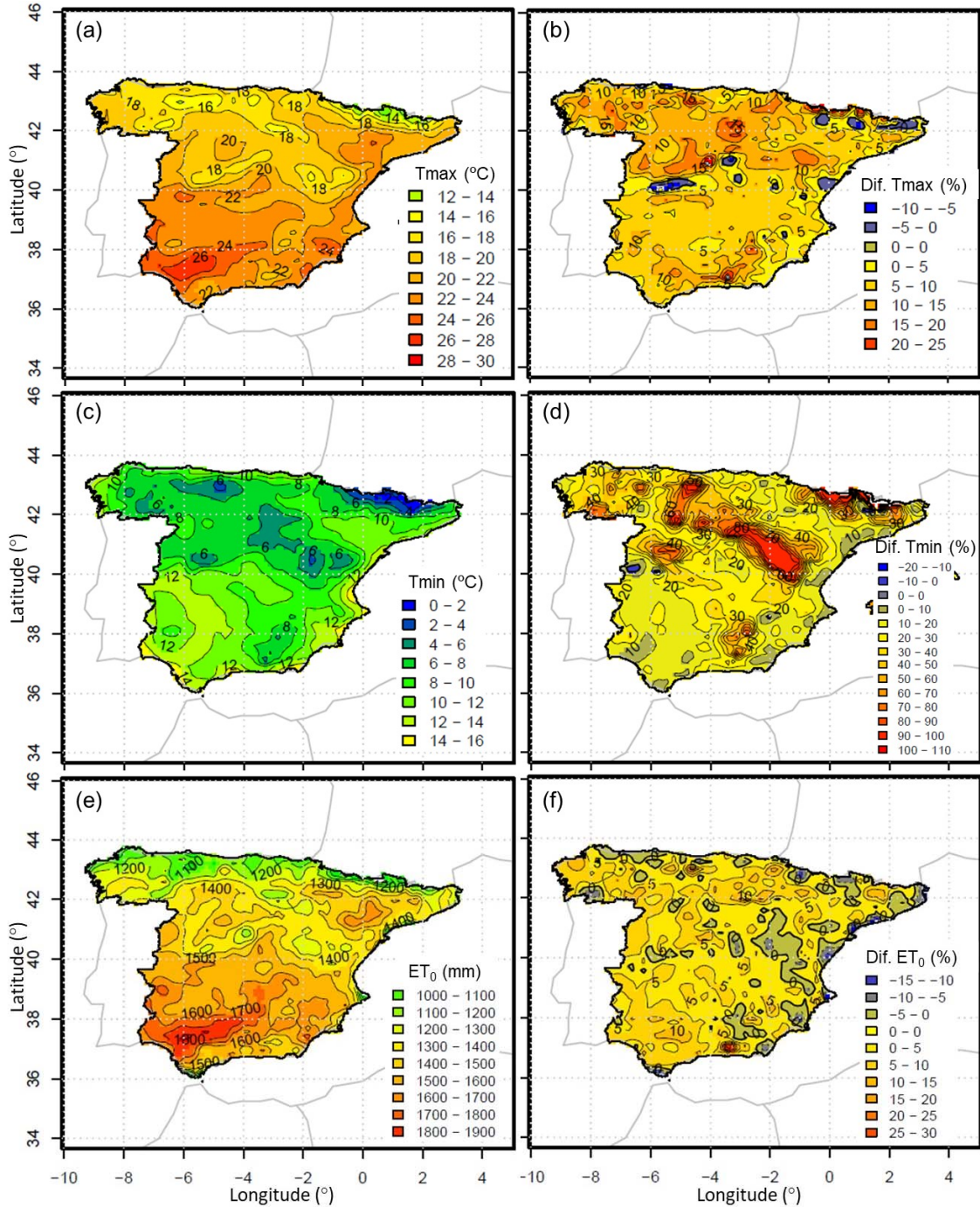


Figure 5. Spatial distribution of: (a,c,e) ensemble of mean annual maximum and minimum temperature, and *ET₀* from RCMs for period 2021–2050; and, (b,d,f) Difference maps (%) between the periods 2021–2050 and 1961–1990 observational dataset, assessed as $[100 \times (\text{mapEns} - \text{mapObs})/\text{mapObs}]$.

The maximum and minimum temperatures (Figure 5a,c) have a spatial distribution with a strong increasing gradient from north to south. The maximum temperature is expected between a minimum

value of 14 °C in the Pyrenees, to values of 26 °C in Andalusia region. South of Spain presents the highest values of minimum temperatures, with maximum values greater than 12 °C, and north of Spain shows the lowest values, with minimum values less than 4 °C in the Pyrenees region.

The map for *ET₀* (Figure 5e) also shows an increasing gradient from north to south, with maximum values of mean *ET₀* (1800 mm) in the southeast of the Spanish territory. From Figure 5b, the maximum temperature is predicted to increase from 10 to 15% in the north of Spain, and from 5 to 10% in the south. While in the Mediterranean coast, increases of 5% are expected. A general increase in the minimum temperature (Figure 5d) between 20 and 30% is expected for the major part of Spain, except for areas of the Mediterranean and Andalusia regions where increases of 10% are expected. While in the Pyrenees and Iberian System are identified the highest increases (greater than 60%). Finally, an increase of mean annual *ET₀* (Figure 5f) from 0 to 5%, reaching 10% in some areas, is predicted for Spain, except for areas of the Mediterranean region.

The variability of the simulated seasonal mean *ET₀* for the three selected areas of Spain: Zone 1, Zone 2, and Zone 3 represented in Figure 1, has been evaluated considering the time reference period observed (1961–1990) and future period (2021–2050). The results are presented in Figure 6.

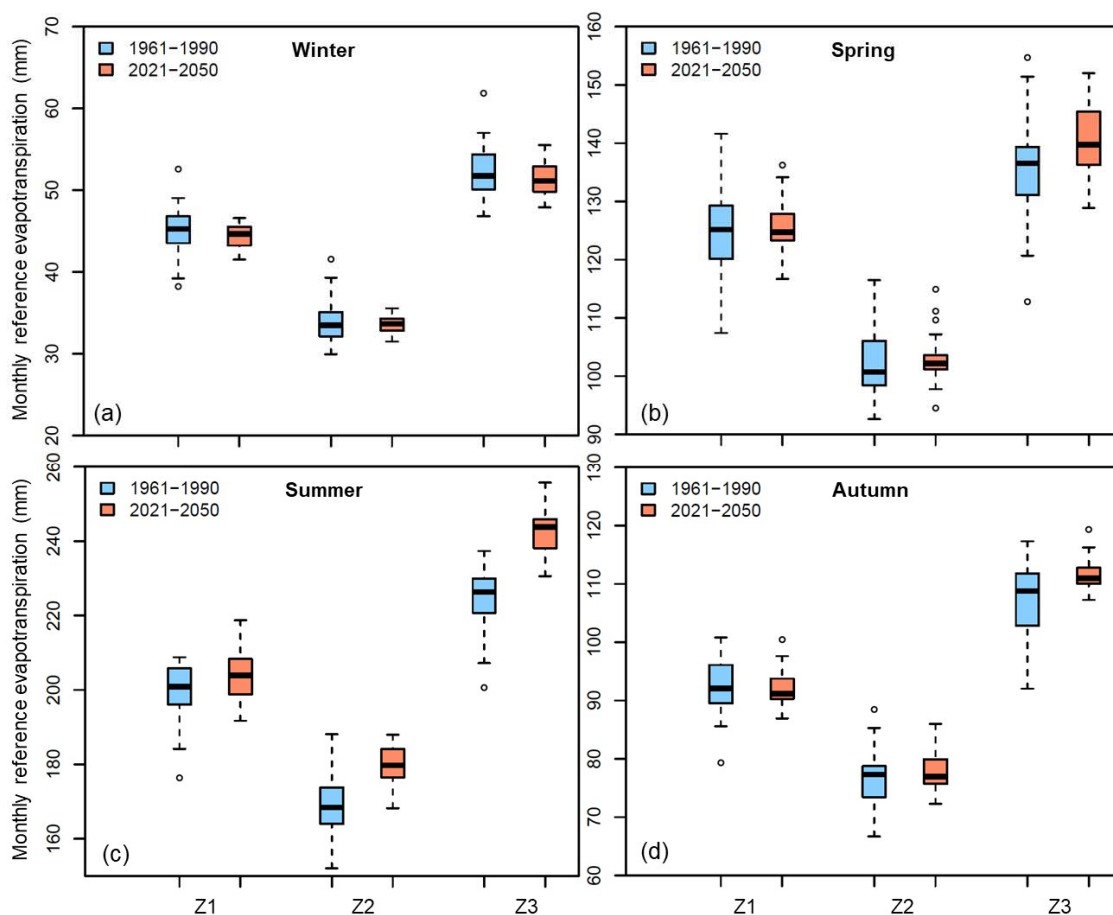


Figure 6. Boxplots of mean *ET₀* simulated for time period 2021–2050 and from observational dataset for time reference period 1961–1990, for the Cantabrian coast (Z1), east of continental Spain (Z2), and Andalusian zone (Z3): (a) Winter, (b) Spring, (c) Summer, and (d) Autumn seasons.

From Figure 6a (winter season) and 6d (autumn season), only slight variations of mean *ET₀* for the future period in comparison to time reference period are projected for the three zones. However, for spring season (Figure 6b), an increase in the mean *ET₀* is expected in Levante zone and also in Andalusian zone. In the case of summer season (Figure 6c), the variation of mean *ET₀* for the future

period is relevant in comparison to time reference period, where the largest increment is expected for the Andalusian region. In conclusion, the major increments of ET_0 values are expected in spring and summer seasons, for the Levante and Andalusia zones.

4. Discussion and Conclusions

Evapotranspiration process returns a high percent of precipitation to the atmosphere over Spain (especially relevant in the South and Southeast of Spain), and it is an important meteorological component when hydrological models are used for projecting future changes on water cycle. Therefore, robust projections of ET_0 , as well as rainfall, are needed to obtain reliable hydrological projections.

The FAO [13] recommend that the Penman-Monteith method could be used as a standard equation to calculate ET_0 . But, the availability of the required information to apply PM method is not enough in some places, such as developing countries or in large areas (e.g., Spain). For this reason, there is a large amount of works in the literature that evaluate the performance of ET_0 equations, that only require temperature and radiation data, against the PM equation [14–18,22,23]. Some authors, like Oudin et al. [7], have demonstrated that the PET formulae based on temperature and radiation tend to provide the best inputs to rainfall–runoff models. For this reason, a simple equation temperature-based ET_0 with few climate variables has been applied to increase the reliability of climate projections. The use of this equation of ET_0 with a calibrated coefficient is supported by works, such as [21–25].

In addition to the uncertainties due to choice the ET_0 method estimation, the selection of the climate model (GCM or RCM) is an important source of uncertainty for future projections of changes, as demonstrated Kingston et al. [42], while comparing six PET methods that were obtained from five different GCMs. However, a large part of the existing works is based on only one RCM or GCM instead of a RCM ensemble. For example, authors such as Obada et al. (2017) [36] have obtained projections of ET_0 in Benin using PM equation for Representative Concentration Pathways scenarios (RCP4.5 and RCP8.5), but only working with three RCMs. The Obada et al. (2017) [36] results indicate that annual ET_0 gradually increase and reach its maximum on 2100.

Zhang et al. [35] have calculated future change in ET_0 with PM equation and projections from three GCMs under A1B and B1 scenarios. These works present some strengths (e.g., they used the PM equation and more than one scenario), but their weaknesses correspond to a low number of climate models and not in consideration of the climate model ensemble.

In comparison with other works, the improvement of the present study is to address the estimation of ET_0 from a RCM ensemble, with the aim to reduce the involved uncertainties. The RCM ensembles of mean, maximum, and minimum temperatures have been built applying a novel methodology that was proposed by [31], based on seasonal and annual variability of these simulated variables from sixteen RCMs (driven by different GCMs for scenario A1B). This methodology has been used successfully in the Southeast of Spain to reduce uncertainties in the runoff projections by Olmos Giménez et al. (2018) [32].

While considering the climate effects of IPCC [39] and RCP scenarios, [43] indicate that the median of the projected warming to the end of the century under the SRES A1B scenario is found between the RCP6 and RCP8.5 scenarios. Moreover, analyzing mean temperature change [44] is found a very high spatial correlation between RCP8.5 and A1B results, with 0.82–0.97 for temperature changes, and even stronger correlation towards the end of the century.

Taking into account the built RCM ensemble of temperatures, the climate projections of ET_0 have been estimated. An increase of seasonal mean ET_0 of 5% due to an increase of maximum and minimum temperatures over Spain, is projected. This increase in ET_0 occurs in summer especially. These results are in line with the trends that were obtained by Vicente-Serrano et al. (2014) [45] for Spain in the time period 1961–2011 by applying various ET_0 estimation equations. The results of the present study are similar to the findings in others regions such as China and West Africa [35,36]. The PET's changes in West Africa are expected from 2 to 7% for 2011–2040 and RCP4.5 and RCP8.5 scenarios [36]. The results of Zhang et al. (2013) [35] show that the air temperature increment would dominate the change in

ET_0 , and ET_0 values will increase for 2050s when compared with the annual mean of period 1960–1990 (increment of 4.42–16.21% for 2050). However, other authors like McVicar et al. (2012) [46] working with trends in observed terrestrial near-surface wind speeds and its implications for evaporation, have uncovered for the last decades the declining rates of evaporative demand (by reviewing papers reporting trends in measured pan evaporation and estimated ET_0).

Finally, the work presents a robust methodology to estimate RCMs ensemble-driven ET_0 projections, and underlines its importance in the study of climate change impacts on hydrological cycle processes, with a reduced requirement of climatic variables.

Author Contributions: The authors contributed equally to the work.

Funding: Fundación Séneca grant number 19527/PI/14.

Acknowledgments: The authors acknowledge the financial support of Fundación Séneca grant number 19527/PI/14, Agency of Science and Technology of Murcia Region in the framework of PCTIRM 2011–2014, Comunidad Autónoma de la Región de Murcia (Spain).

Conflicts of Interest: The authors declare no conflict of interest.

References

1. Paredes, D.; Trigo, R.M.; García-Herrera, R.; Franco Trigo, I. Understanding precipitation changes in Iberia in early spring: Weather typing and storm-tracking approaches. *J. Hydrometeorol.* **2006**, *7*, 101–113. [CrossRef]
2. Solomon, S.; Qin, D.; Manning, M.; Chen, Z.; Marquis, M.; Averyt, K.; Tignor, M.; Miller, H. Climate Change 2007: The Physical Science Basis. In *Contribution of Working Group I to the Fourth Assessment Report of the Intergovernmental Panel on Climate Change*; Solomon, S., Qin, D., Manning, M., Chen, Z., Marquis, M., Averyt, K.B., Tignor, M., Miller, H.L., Eds.; Cambridge University Press: New York, NY, USA, 2007.
3. Giraldo Osorio, J.D.; García Galiano, S.G. Assessing uncertainties in the building of ensemble RCMs over Spain based on dry spell lengths probability density functions. *Clim. Dyn.* **2013**, *40*, 1271–1290. [CrossRef]
4. Prudhomme, C.; Williamson, J. Derivation of RCM-driven potential evapotranspiration for hydrological climate change impact analysis in Great Britain: A comparison of methods and associated uncertainty in future projections. *Hydrol. Earth Syst. Sci.* **2013**, *17*, 1365–1377. [CrossRef]
5. Oudin, L.; Hervieu, F.; Michel, C.; Perrin, C.; Andréassian, V.; Anctil, F.; Loumagne, C. Which potential evapotranspiration input for a lumped rainfall–runoff model? Part 2—Towards a simple and efficient potential evapotranspiration model for rainfall–runoff modelling. *J. Hydrol.* **2005**, *303*, 290–306. [CrossRef]
6. Bai, P.; Liu, X.; Yang, T.; Li, F.; Liang, K.; Hu, S.; Liu, C. Assessment of the influences of different potential evapotranspiration inputs on the performance of monthly hydrological models under different climatic conditions. *J. Hydrometeorol.* **2016**, *17*, 2259–2274. [CrossRef]
7. Lang, D.; Zheng, J.; Shi, J.; Liao, F.; Ma, X.; Wang, W.; Chen, X.; Zhang, M. A Comparative Study of Potential Evapotranspiration Estimation by Eight Methods with FAO Penman–Monteith Method in Southwestern China. *Water* **2017**, *9*, 734. [CrossRef]
8. Doorenbos, J.; Pruitt, W.O. *Guidelines for Predicting Crop Water Requirements*; FAO Irrigation and Drainage Paper 24; Food and Agricultural Organization of the United Nations: Rome, Italy, 1977. Available online: <http://www.fao.org/3/a-f2430e.pdf> (accessed on 20 January 2018).
9. Martínez Pérez, J.A.; García-Galiano, S.G.; Martín-Gorriz, B.; Baille, A. Satellite-Based Method for Estimating the Spatial Distribution of Crop Evapotranspiration: Sensitivity to the Priestley–Taylor Coefficient. *Remote Sens.* **2017**, *9*, 611. [CrossRef]
10. Hetzroni, A.; Peters, A.; Ben-Gal, A. Towards precision management of orchards: Using automated monitoring to build a GIS-based spatial decision support system. In *Proceedings of the International Conference on Agricultural Engineering, Valencia, Spain, 8–12 July 2012*.
11. Douglas, E.M.; Beltrán-Przekurat, A.; Niyogi, D.; Pielke, R.A.; Vorosmarty, C.J. The impact of agricultural intensification and irrigation on land–atmosphere interactions and Indian monsoon precipitation—A mesoscale modeling perspective. *Glob Planet. Chang.* **2009**, *67*, 117–128. [CrossRef]
12. Katerji, N.; Rana, G. Crop reference evapotranspiration: a discussion of the concept, analysis of the process and validation. *Water Resour. Manag.* **2011**, *25*, 1581–1600. [CrossRef]

13. Allen, R.G.; Pereira, L.S.; Raes, D.; Smith, M. *Crop Evapotranspiration-Guidelines for Computing Crop Water Requirements-FAO Irrigation and Drainage Paper 56*; FAO: Rome, Italy, 1998.
14. Djaman, K.; Balde, A.B.; Sow, A.; Muller, B.; Irmak, S.; N'Diaye, M.K.; Manneh, B.; Moukoumbi, Y.D.; Futakuchi, K.; Saito, K. Evaluation of sixteen reference evapotranspiration methods under sahelian conditions in the Senegal River Valley. *J. Hydrol. Reg. Stud.* **2015**, *3*, 139–159. [[CrossRef](#)]
15. Tabari, H. Evaluation of reference crop evapotranspiration equations in various climates. *Water Resour. Manag.* **2010**, *24*, 2311–2337. [[CrossRef](#)]
16. Samaras, D.A.; Reif, A.; Theodoropoulos, K. Evaluation of Radiation-Based Reference Evapotranspiration Models under Different Mediterranean Climates in Central Greece. *Water Resour. Manag.* **2014**, *28*, 207–225. [[CrossRef](#)]
17. Tegos, A.; Malamos, N.; Koutsoyiannis, D. A parsimonious regional parametric evapotranspiration model based on a simplification of the Penman–Monteith formula. *J. Hydrol.* **2015**, *524*, 708–717. [[CrossRef](#)]
18. Hargreaves, G.H.; Samani, Z.A. Reference crop evapotranspiration from temperature. *Appl. Eng. Agric.* **1985**, *1*, 96–99. [[CrossRef](#)]
19. Droogers, P.; Allen, R.G. Estimating reference evapotranspiration under inaccurate data conditions. *Irrig. Drain. Syst.* **2002**, *16*, 33–45. [[CrossRef](#)]
20. Xu, C.Y.; Singh, V.P. Cross comparison of empirical equations for calculating potential evapotranspiration with data from Switzerland. *Water Resour. Manag.* **2002**, *16*, 197–219. [[CrossRef](#)]
21. Martínez-Cob, A.; Tejero-Juste, M. A wind-based qualitative calibration of the Hargreaves ETo estimation equation in semiarid regions. *Agric. Water Manag.* **2004**, *64*, 251–264. [[CrossRef](#)]
22. Trajkovic, S. Hargreaves versus Penman-Monteith under humid conditions. *J. Irrig. Drain. Eng.* **2007**, *133*, 38–42. [[CrossRef](#)]
23. Maestre-Valero, J.F.; Martínez-Álvarez, V.; González Real, M.M. Regionalization of the Hargreaves coefficient to estimate long-term reference evapotranspiration series in SE Spain. *Span. J. Agric. Res.* **2013**, *11*, 1137–1152. [[CrossRef](#)]
24. Shahidian, R.; Serralheiro, P.; Serrano, J.; Teixeira, J.L. Parametric calibration of the Hargreaves–Samani equation for use at new locations. *Hydrol. Process.* **2013**, *27*, 605–616. [[CrossRef](#)]
25. Shiri, J.; Sadraddini, A.A.; Nazemi, A.H.; Marti, P.; Fard, A.F.; Kisi, O.; Landaras, G. Independent testing for assessing the calibration of the Hargreaves–Samani equation: New heuristic alternatives for Iran. *Comput. Electron. Agric.* **2015**, *117*, 70–80. [[CrossRef](#)]
26. Tegos, A.; Malamos, N.; Efstratiadis, A.; Tsoukalas, I.; Karanasios, A.; Koutsoyiannis, D. Parametric Modelling of Potential Evapotranspiration: A Global Survey. *Water* **2017**, *9*, 795. [[CrossRef](#)]
27. Christensen, J.; Kjellstrom, E.; Giorgi, F.; Lenderink, G.; Rummukainen, M. Weight assignment in regional climate models. *Clim. Res.* **2010**, *44*, 179–194. [[CrossRef](#)]
28. Karambiri, H.; García Galiano, S.G.; Giraldo, J.D.; Yacouba, H.; Ibrahim, B.; Barbier, B.; Polcher, J. Assessing the impact of climate variability and climate change on runoff in West Africa: The case of Senegal and Nakambe River basins. *Atmos. Sci. Lett.* **2011**, *12*, 109–115. [[CrossRef](#)]
29. Giorgi, F.; Mearns, L.O. Calculation of average, uncertainty range, and reliability of regional climate changes from AOGCM simulations via the “reliability ensemble averaging” (REA) method. *J. Clim.* **2002**, *15*, 1141–1158. [[CrossRef](#)]
30. Paeth, H.; Hall, N.M.J.; Gaertner, M.; Alonso, M.D.; Moumouni, S.; Polcher, J.; Ruti, P.M.; Fink, A.H.; Gosset, M.; Lebel, T.; et al. Progress in regional downscaling of west African precipitation. *Atmos. Sci. Lett.* **2011**, *12*, 75–82. [[CrossRef](#)]
31. Olmos Giménez, P.; García Galiano, S.G.; Giraldo Osorio, J.D. Identifying a robust method to build RCMs ensemble as climate forcing for hydrological impact models. *Atmos. Res.* **2016**, *174–175*, 31–40. [[CrossRef](#)]
32. Olmos Giménez, P.; García Galiano, S.G.; Giraldo Osorio, J.D. Improvement of Hydroclimatic Projections over Southeast Spain by Applying a Novel RCM Ensemble Approach. *Water* **2018**, *10*, 52. [[CrossRef](#)]
33. Xu, C.H.; Xu, Y. The projection of temperature and precipitation over China under RCP scenarios using a CMIP5 multi-model ensemble. *Atmos. Ocean. Sci. Lett.* **2012**, *5*, 527–533. [[CrossRef](#)]
34. Diallo, I.; Sylla, M.B.; Giorgi, F.; Gaye, A.T.; Camara, M. Multimodel GCM-RCM Ensemble-Based Projections of Temperature and Precipitation over West Africa for the Early 21st Century. *Int. J. Geophys.* **2012**, *2012*, 972896. [[CrossRef](#)]

35. Zhang, D.; Liu, X.; Hong, H. Assessing the effect of climate change on reference evapotranspiration in China. *Stoch. Environ. Res. Risk Assess.* **2013**, *27*, 1871. [[CrossRef](#)]
36. Obada, E.; Alamou, E.A.; Chabi, A.; Zandagba, J.; Afouda, A. Trends and Changes in Recent and Future Penman-Monteith Potential Evapotranspiration in Benin (West Africa). *Hydrology* **2017**, *4*, 38. [[CrossRef](#)]
37. Herrera, S.; Gutiérrez, J.M.; Ancell, R.; Pons, M.R.; Frías, M.D.; Fernández, J. Development and analysis of a 50-year high-resolution daily gridded precipitation dataset over Spain (Spain02). *Int. J. Climatol.* **2012**, *32*, 74–85. [[CrossRef](#)]
38. Christensen, J.H.; Rummukainen, M.; Lenderink, G. *Formulation of Very High-Resolution Regional Climate Model Ensembles for Europe. ENSEMBLES: Climate Change and Its Impacts at Seasonal, Decadal and Centennial Timescales: Summary of Research and Results from the ENSEMBLES Project*; Van der Linden, P., Mitchell, J.F.B., Eds.; Met Office Hadley Centre: London, UK, 2009; pp. 47–58.
39. Intergovernmental Panel on Climate Change (IPCC). *Special Report on Emissions Scenarios: A Special Report of Working Group III of the Intergovernmental Panel on Climate Change*; Nakićenović, N., Swart, R., Eds.; Cambridge University Press: Cambridge, UK, 2000.
40. Giorgi, F.; Mearns, L.O. Probability of regional climate change based on reliability ensemble averaging (REA) method. *Geophys. Res. Lett.* **2003**, *30*, 311–314. [[CrossRef](#)]
41. Sheskin, D.J. *Handbook of Parametric and Nonparametric Statistical Procedures*, 2nd ed.; Chapman & Hall, CRC: Boca Raton, FL, USA, 2000.
42. Kingston, D.; Todd, M.; Taylor, R.G.; Thompson, J.R.; Arnell, N.W. Uncertainty in the estimation of potential evapotranspiration under climate change. *Geophys. Res. Lett.* **2009**, *36*, L20403. [[CrossRef](#)]
43. Zittis, G.; Hadjinicolaou, P.; Fnais, M.; Lelieveld, J. Projected changes in heat wave characteristics in the eastern Mediterranean and the Middle East. *Reg. Environ. Chang.* **2016**, *16*, 1863–1876. [[CrossRef](#)]
44. Jacob, D.; Petersen, J.; Eggert, B.; Alias, A.; Christensen, O.B.; Bouwer, L.M.; Braun, A.; Colette, A.; Déqué, M.; Georgievski, G.; et al. EURO-CORDEX: New high-resolution climate change projections for European impact research. *Reg. Environ. Chang.* **2014**, *14*, 563–578. [[CrossRef](#)]
45. Vicente-Serrano, S.M.; Azorin-Molina, C.; Sanchez-Lorenzo, A.; Revuelto, J.; López-Moreno, J.I.; González-Hidalgo, J.C.; Moran-Tejeda, E.; Espejo, F. Reference evapotranspiration variability and trends in Spain, 1961–2011. *Glob. Planet. Chang.* **2014**, *121*, 26–40. [[CrossRef](#)]
46. McVicar, T.R.; Roderick, M.L.; Donohue, R.J.; Li, L.T.; Van Niel, T.G.; Thomas, A.; Grieser, J.; Jhajharia, D.; Himri, Y.; Mahowald, N.M.; et al. Global review and synthesis of trends in observed terrestrial near-surface wind speeds: Implications for evaporation. *J. Hydrol.* **2012**, *416–417*, 182–205. [[CrossRef](#)]



© 2018 by the authors. Licensee MDPI, Basel, Switzerland. This article is an open access article distributed under the terms and conditions of the Creative Commons Attribution (CC BY) license (<http://creativecommons.org/licenses/by/4.0/>).